Analysis of hyperfine structure in chalcogen-doped silicon and germanium nanowires

Guido Petretto*
Laboratorio MDM, IMM - CNR via C. Olivetti, 2 20864 Agrate Brianza (MB), Italy;
Dipartimento di Scienza dei Materiali, Università degli Studi di Milano-Bicocca, via Cozzi 53, 20125 Milano, Italy;
and Institute of Condensed Matter and Nanosciences, Université catholique de Louvain, Chemin des étoiles 8, bte L7.03.01, 1348 Louvain-la-Neuve, Belgium

Andrea Massé† and Marco Fanciulli
Laboratorio MDM, IMM - CNR via C. Olivetti, 2 20864 Agrate Brianza (MB), Italy
and Dipartimento di Scienza dei Materiali, Università degli Studi di Milano-Bicocca, via Cozzi 53, 20125 Milano, Italy

Alberto Debernardi‡
Laboratorio MDM, IMM - CNR via C. Olivetti, 2 20864 Agrate Brianza (MB), Italy
(Received 17 November 2014; revised manuscript received 3 February 2015; published 24 March 2015)

Due to the confinement effect, the donor wave functions in nanostructures are highly localized on the defect and can even be deformed by the local geometry of the system. This can have relevant consequences on the hyperfine structure of the defect that can be exploited for advanced electronic applications. In this work we employ *ab initio* density functional calculations to explore the hyperfine structure of S and Se substitutional defects in silicon and germanium nanowires. We show that, if the tetrahedral symmetry is preserved, the hyperfine contact term is only marginally dependent on the nanowire orientation, while it can undergo drastic changes if the symmetry is lost. In addition, we provide an analysis of the strain dependence of the hyperfine structure for the different orientations of the nanowires.

DOI: 10.1103/PhysRevB.91.125430 PACS number(s): 81.07.Gf, 61.72.J−, 31.30.Gs

I. INTRODUCTION

In recent years, semiconductor nanowires have gained increasing importance since they are promising one-dimensional nanostructures for future applications in the field of nanoelectronics. This is due to their reduced sizes and to the fact that physical confinement along two directions allows us to control the band gap of such nanostructures, and, consequently, to tune important properties like the conductivity and the photoluminescence. In addition, their electronic properties can be controlled by introducing *p*- and *n*-type dopants during synthesis. For this reason, semiconductor nanowires are interesting building blocks for the production of nanodevices [1,2], such as field-effect transistors [3], LEDs [4], lasers [5], and photovoltaic cells [6,7].

For pristine and doped silicon nanowires (SiNWs) the electronic properties have been studied extensively from both theoretical and experimental points of view [8,9], demonstrating the importance of the effect of quantum confinement [10]. Germanium nanowires (GeNWs) have received less attention than their Si counterpart, but similar effects have been observed [11,12]. In addition, silicon-germanium nanowires have also been considered as promising components for microelectronic devices [13]. These can be prepared as alloyed nanowires or as axial and radial heterostructures, which, when doped, can be useful due to their band offset [14].

Given the relevance of doping in the two materials and in their heterostructures, it is interesting to push forward the analysis on doped nanowires. In fact, besides introducing electronic levels, donor defects can give rise to a strong hyperfine interaction. The importance of this aspect resides in the fact that donors with a large hyperfine contact term might be employed for the development of nuclear spin based quantum computers [15–17]. In particular, in doped semiconductor nanostructures it is possible to observe a consistent increase of the defect contact term, as a consequence of quantum confinement. This kind of behavior has been confirmed both by theoretical calculations [18–20] and electron paramagnetic resonance (EPR) experiments [21] for group V dopants in silicon nanocrystals, while only theoretical calculations for P [22] and Se [23] doped SiNWs are available at the moment.

In the context of the development of nuclear spin based quantum bits, chalcogen defects have been suggested as good doping elements, even for bulk crystals, since they are characterized by a lower extension of the donor wave function, and therefore, can present a larger contact term even in bulk materials [16,24].

In order to support the feasibility of this kind of approach and to provide further information to be compared with experimental results, we have considered the case of chalcogen doping in silicon and germanium nanowires. More in detail, we studied SiNWs and GeNWs characterized by different diameters and orientations, and doped with selenium or sulfur atoms, located in the core region of the nanowire. In the following we will show that the trend of the hyperfine contact term as a function of the diameter is in agreement with the theory of quantum confinement, and that the contact term is also very sensitive to the local structure around the defect, i.e., a breaking of the local symmetry of the defect alters the trend

*guido.petretto@mdm.imm.cnr.it
†Present address: Department of Applied Physics, Eindhoven University of Technology, P.O. Box 513, 5600 MB Eindhoven, The Netherlands.
‡alberto.debernardi@mdm.imm.cnr.it

of the contact term as a function of nanostructure size. We will also present a detailed analysis of the effect of compressive and tensile strain on the hyperfine parameters for Se doped SiNWs, highlighting common features and differences among the three orientations considered.

II. COMPUTATIONAL DETAILS

All calculations have been performed using the open-source suite QUANTUM-ESPRESSO [25], based on density functional theory (DFT), plane waves, and pseudopotentials methods. We chose the generalized gradient approximation (GGA) as proposed by Perdew, Burke, and Ernzerhof [26] as an exchange-correlation functional for silicon, whereas the local density approximation (LDA), as proposed by Perdew and Zunger [27], was used for germanium. This choice is justified by the fact that unlike bulk silicon, for which the GGA provides the widest band gap ($E_g = 0.64$ eV), within our approximations bulk germanium has a zero band gap in the GGA, while a small one ($E_g = 0.41$ eV) is opened using the LDA [28,29].

The choice of the exchange-correlation functional used to describe the system could also be considered critical because, as pointed out by Niquet *et al.* [30], (semi) local approximations fail to correctly describe the impurity when dealing with the highest occupied molecular orbital (HOMO) of the neutral system, while correct results should be obtained studying the lowest unoccupied molecular orbital (LUMO) of the ionized system. It could then be argued that the total spin density, the key element to determine the hyperfine parameters, would mainly depend on the HOMO of the system, thus leading to flawed results. However, we have shown that when it comes to the shape of the donor wave function the overall relation between the different orientations is preserved and the differences in the treatment with the HOMO and LUMO methods are particularly small in the close vicinity of the donor [31]. Since this is all that matters in our calculations, we conclude that the results presented in the paper should provide a good approximation for the expected hyperfine parameters in ultrathin Si and Ge nanowires.

All the pseudopotentials employed for the simulations are norm conserving of the Troullier-Martins type [32]. The kinetic energy cutoff has been set to 40 Ry for silicon and of 50 Ry for germanium. However, since the calculation of the hyperfine parameters requires the knowledge of the electron spin density close to the nucleus, we have used the projector augmented wave (PAW) method in order to reconstruct the real wave function from the pseudowave function obtained after the self-consistent calculation [33]. This is implemented through the GIPAW formalism [34]. Moreover, since the calculation of hyperfine parameters involves singly ionized double donors, we used spin polarization calculations with total magnetization of $+1$.

Structural relaxations were performed until the forces on all atoms were lower than 0.02 eV/Å. We considered a separation of at least 10 Å between the periodic replicas of each nanowire, and a Monkhorst-Pack $1 \times 1 \times N$ k-point grid for surface Brillouin zone integration [35], where N depends on the length of the supercell and on the type of nanowire material, so to keep approximately the same k-point grid along the growth direction. In order to minimize the fictitious interaction between a defect and its replicas, we chose a supercell length of about 1.6 nm along the growth direction for doped nanowires. Nanowire structures have been obtained by cutting from bulk silicon and bulk germanium cylinders of different diameters oriented along the [001], [011], and [111] directions. The nanowires considered here have a diameter that ranges from approximately 0.8 to 2.0 nm, where the diameter is defined as the average of the radial coordinate of the surface silicon or germanium atoms. The nine studied structures are shown in Fig. 1.

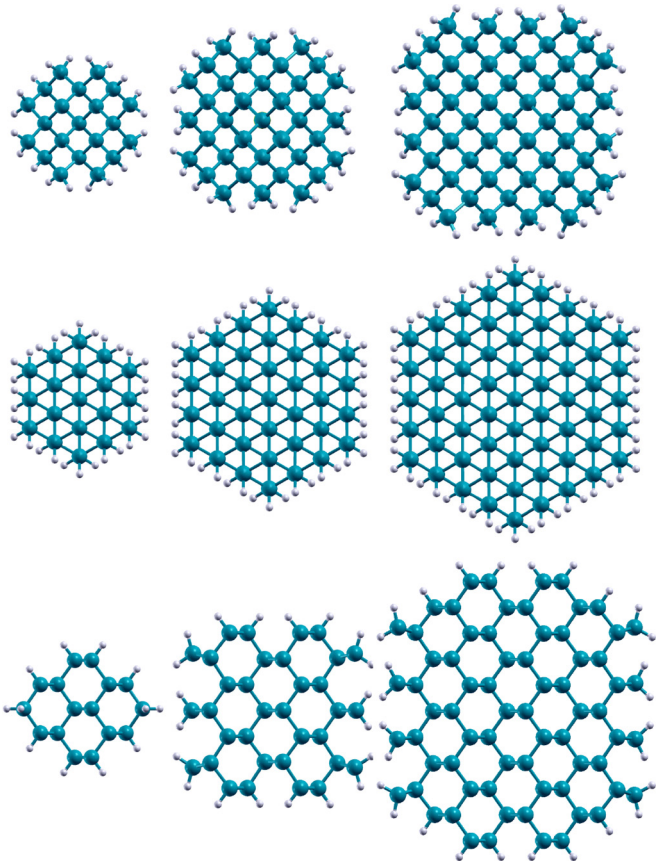

FIG. 1. (Color online) Cross sections of the nanowires considered for [001] (first row), [111] (second row), and [011] (third row) orientations. Blue spheres represent Si and Ge, while white spheres are the H passivating atoms. The diameters range from 0.8 nm for the smallest to 2.0 nm for the largest nanowires.

It should be noted that the structure considered for the [011] orientation present some peculiarities, compared to the other orientations. One is given by the displacement of the passivating atoms that can lead to a large strain caused by the possible presence of two H atoms at a small distance that repel each other. This is actually the case for the smaller [011] nanowire considered and the lattice parameter results to be slightly larger along the axis, compared to the other nanowires. To partially reduce this effect we have considered here a canted dihydride passivation for this nanowire, which also proved to be more stable [36,37]. This is of particular importance since it has been demonstrated that the delocalization of the donor wave function is much larger for [011] nanowires compared to the other orientations and that this property is particularly sensitive to the strain [31]. In order to avoid this effect, the

other [011] nanowires considered here have been constructed in such a way to avoid the presence of H passivating atoms at small distances.

Concerning the position of the impurities, the choice of considering only the sites in the core region of the nanowires has been motivated with the aim of isolating the effect of different orientations and different dopants from those of the interaction with the surface and with passivating atoms that can give rise to strong deformations [23]. This can provide a term of comparison with experimental data, since uniformly doped nanowires have been synthesized [38].

III. HYPERFINE PARAMETERS

In the presence of a defect in a solid with unpaired electrons, the hyperfine interaction is defined as the interaction between the magnetic moment of the electron with the magnetic moments of the nuclei. The hyperfine Hamiltonian is given by

$$\hat{H} = \hat{\mathbf{S}} \cdot \mathbf{A} \cdot \hat{\mathbf{I}}, \tag{1}$$

where $\hat{\mathbf{S}}$ is the electron spin operator, $\hat{\mathbf{I}}$ is the nuclear spin operator, and $\mathbf{A}$ is a tensor describing the hyperfine coupling. In this context, the interaction of the electron spin density is referred to as hyperfine interaction (HFI) when $\hat{\mathbf{I}}$ is the spin of the donor nucleus and superhyperfine interaction (SHFI) when it is the spin of the neighbor nuclei.

The coupling constant $\mathbf{A}$ of the Hamiltonian in Eq. (1) can be divided into two terms:

$$\mathbf{A} = a\mathbf{1} + \mathbf{A}_{\text{dip}}. \tag{2}$$

Here a is the scalar Fermi-contact term that is obtained from the isotropic part of the Hamiltonian and is a measure of the amount of the electron spin density at the nucleus, while the second term originates from the dipole-dipole interaction and depends on the anisotropic part of the electronic spin density.

The dipolar term $\mathbf{A}_{\text{dip}}$ is, by definition, a traceless tensor and is diagonal in the hyperfine principal axis system. Hence, it is usually defined by two independent parameters in the standard form

$$\mathbf{A}_{\text{dip}} = \begin{pmatrix} -b + b' & 0 & 0 \\ 0 & -b - b' & 0 \\ 0 & 0 & 2b \end{pmatrix}, \tag{3}$$

where b and b' are called uniaxiality and asymmetry, respectively. These parameters vanish for substitutive defects in Si and Ge bulk crystals due to the lattice symmetries and thus nonzero values signal a symmetry breaking at the defect site.

We refer to our earlier paper [23] for more details about the calculations of the hyperfine terms. Note also that the data for the Se doped [001] SiNWs and bulk Si provided in the following are taken from the same reference.

In Fig. 2 the hyperfine contact term a is shown as a function of the nanowire diameter for the different materials, dopants, and orientations considered. The calculated values of a in bulk crystals are shown as well. These represent the values to whom the nanowire results should converge in the limit of large diameters. When available we can compare these values with experimental data to evaluate the quality of our approximations. In bulk silicon, the contact term amounts to

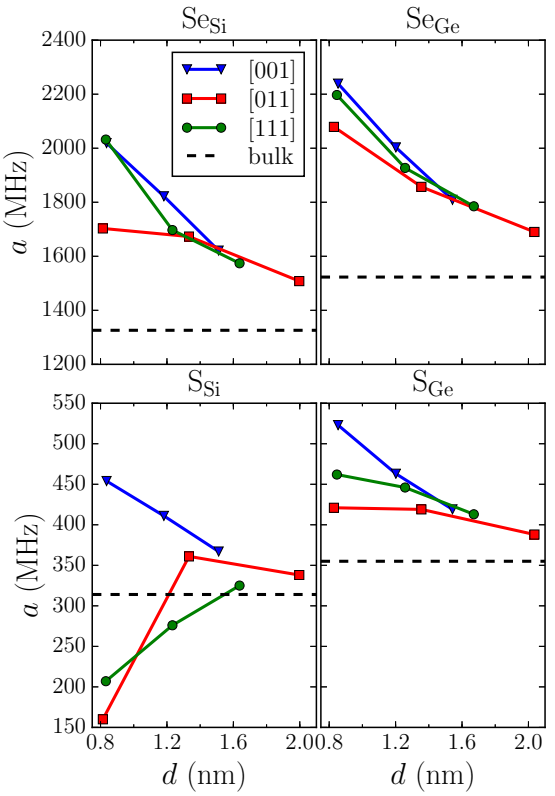

FIG. 2. (Color online) Hyperfine contact term a as a function of the nanowire diameter for [001], [001], and [111] SiNWs (left) and GeNWs (right), doped with Se (top) and S (bottom). The horizontal dashed line represents the bulk value as calculated within our approximations. Data for [001] orientation and bulk in top left panel are from Ref. [23].

1658 MHz for Se [39] and 312 MHz for S [40] and our results are 1327 and 314 MHz, respectively, showing that we can achieve a fair agreement with electron paramagnetic resonance measurements.

The calculated values in bulk germanium are 1523 MHz for Se and 355 MHz for S. These are only slightly larger than those in silicon, and, as we will show, the same ratio between the two materials is preserved also for S and Se defects in nanowires with similar radii, in the cases where the symmetries of the system are preserved. Since the differences in the values of a between the SiNWs and the corresponding GeNWs are significantly lower than those due to size changing, we conclude that a simple measurement of the hyperfine parameters will not be helpful in determining the defect host material in SiGe heterostructures, as, e.g., core shell SiGe nanowires.

With the exception of S in [011] and [111] oriented SiNWs, the main effect of the physical confinement is that of squeezing the donor wave function towards the impurity, leading, in the range of diameters that we have explored, to an almost linear increase of a when reducing the nanowire diameter d.

Let us focus first on the Se doped nanowires. Apart from the smallest [011] SiNW, it can be immediately seen that the contact term is almost independent of the nanowire orientation, suggesting that the effect of physically confining the donor wave function on the defect site is almost the same for all the

orientations and dominates over other effects, like for example those coming from different faceting of the nanowires. This is true for both SiNWs and GeNWs.

However, we can see that, while for the largest [011] nanowires the values of a seems to fit the general trend, for the two smaller sizes the values are always slightly smaller than those for other orientations. This is an immediate consequence of the larger delocalization of the donor wave function along the axis of the nanowire for this orientation compared to the others [31]. The larger delocalization thus comes at the price of a relatively small reduction of the hyperfine contact term. This should be taken into account in light of possible applications, like spin qubits that require large values of a [24,41]. More details about this effect can be recognized in relation with the strain that we will discuss in the next section.

The interpretation for sulfur doped nanowires is less straightforward, in particular for SiNWs. In fact, while for [001] oriented nanowires the symmetries of the systems tend to be preserved, leading, like in the case of Se, to a linear dependence of a as a function of d, the other results are altered by a quite strong breaking of the defect symmetry. In this case, the S atom in the +1 charge state tends to have shorter bonds with three of its four Si nearest neighbors. This effect is probably due to the smaller atomic radius of sulfur compared to selenium. We note, however, that in Ref. [23] we observed a similar behavior for Se doped nanowires, when the defect is close to the surface. This symmetry breaking can thus be induced on chalcogen defects when the lattice has a way to release the strain and does not strongly enforce the tetrahedral symmetry on the defect.

The alteration of the local symmetry at the defect site results in a deformation of the donor wave function that lowers the hyperfine contact term even below the bulk value limit, nullifying the effect of confinement. These deformations are nonetheless possible because of the small size of the nanowires considered, where the defects are relatively close to the surface, even if they are in the nanowire core region. In fact, as soon as the diameter is increased, the asymmetries are reduced or eliminated and the values of the contact term tends to revert to those corresponding to the linear decrease as a function of d.

The anisotropic part of the hyperfine interaction will not be discussed in detail for all the nanowires that we have

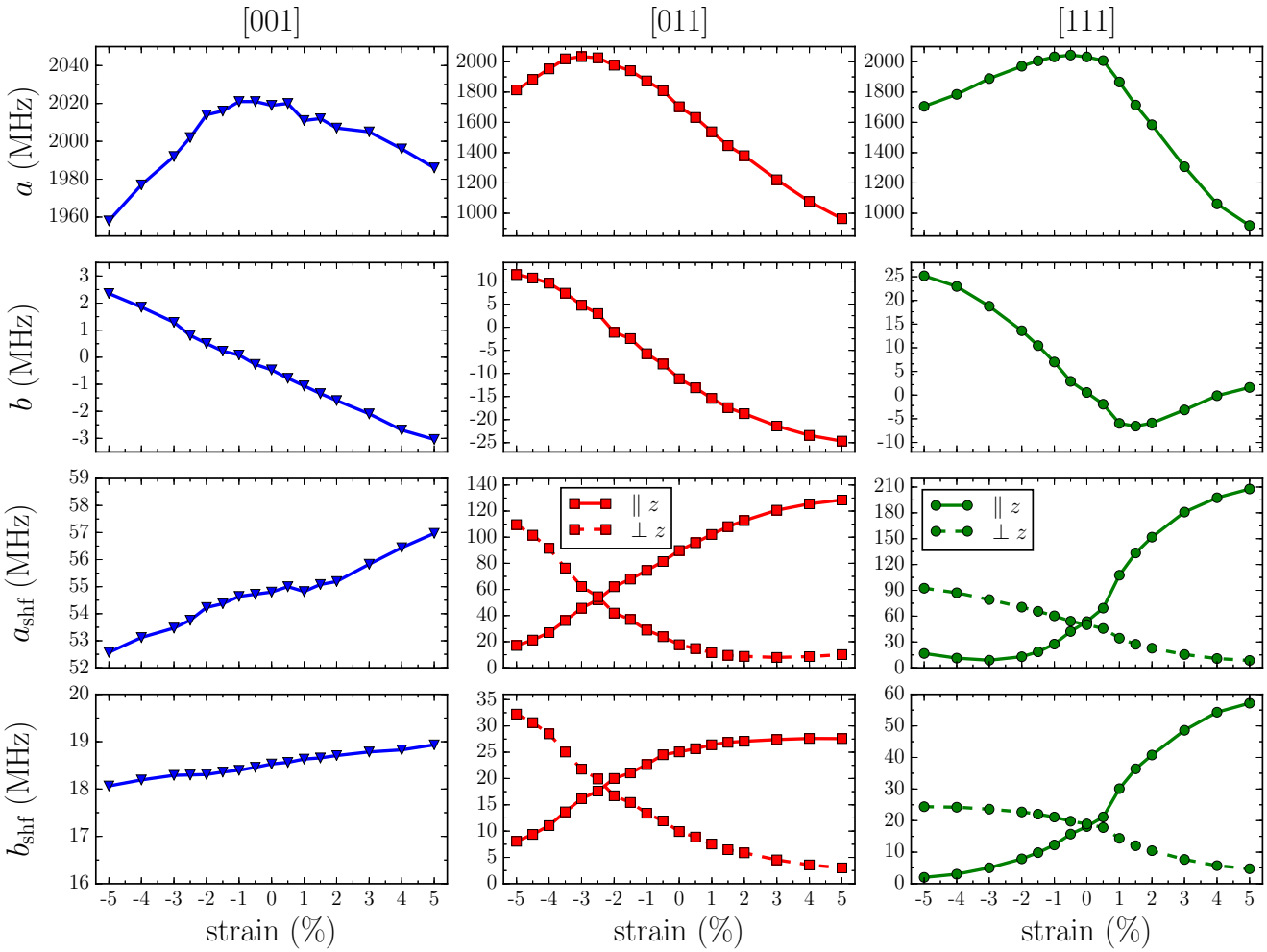

FIG. 3. (Color online) Hyperfine contact term a, anisotropic term b, and nearest neighbor superhyperfine contact term a_{shf} and anisotropic term b_{shf}, for the smallest Se doped SiNWs considered, as a function of applied uniaxial strain. The strain is expressed as a percentage variation with respect to the relaxed supercell size along the nanowire axis. The values of a_{shf} and b_{shf} are obtained as averages of equivalent nearest neighbor. For [011] and [111] nanowires the results are separated depending on whether the bonds of the Si atoms with the defect are oriented along ($\parallel z$) or perpendicularly ($\perp z$) to the nanowire axis.

considered. In fact, the b and b' terms, representing the deviation from the tetrahedral symmetry, are usually smaller than 1 MHz, and quite close to zero, except for the cases discussed above, where the symmetry is strongly reduced. In particular, b' is even smaller than b, due to the fact that it represents the departing from the axial symmetry, which tends to be preserved in a cylindrical structure. In light of this, we will not further discuss its values. In our case, the values of these two parameters are anyway much smaller than those that can be obtained from other defects, like vacancies and vacancy complexes in silicon [42,43]. Also, as will be made clear in the next section, these small quantities are too sensitive to small changes in the supercell length and thus do not provide reliable information to be compared with experimental data, apart from their order of magnitude.

IV. STRAIN EFFECT

In order to characterize and better understand these results, we have studied the effects of uniaxial strain applied along the axis of the nanowires with different orientations. Here we have limited the analysis to the case of Se doped SiNWs with the smallest radius considered. In fact, this set of nanowires display local symmetries similar to those present in the larger ones and can thus provide a reliable model to extract general trends, as long as the defect positions are limited to the core region of the nanowires.

The results of the strain dependence of the hyperfine parameters for the different orientations are collected in Fig. 3. We have covered a range of applied strain from -5% to $+5\%$, which corresponds to the reported experimental limit sustainable by small SiNWs [44]. In the neighborhood of the unstrained system and where the results undergo a change of trend a fine grid of 0.5% has been used, while at larger strain, where the trends are well established, we have limited to a coarser grain of 1%. For [001] and [111] nanowires the most relevant interval is between -2% and $+2\%$, while for [011] it is important to consider carefully even a larger compressive strain. This is due to the fact that the lattice parameter along the growth direction of the [011] nanowire is larger than the ones of [001] and [111] nanowires, as discussed in Sec. II, and this shifts the position of the maximum of a.

First, we use the effect of strain to test the reliability of our results with respect to the supercell size. If we consider a small range around the unstrained configuration, from Fig. 3 it can be seen that the contact term a has extremely small variations for the [001] and [111] orientations. Even for the [011] orientation, where the change is sizable, a variation of 0.5% in the supercell length amounts to a change in the value of around 5%. This demonstrates that the results discussed before will not be affected by possible small imprecisions in reproducing the correct lattice parameters. On the other hand, the anisotropic term b has always a linear dependence on the applied strain and a variation of 0.5% in the supercell length can change its value by more than 50%. Even a tiny change in the local symmetry can thus alter considerably the value of b. We conclude that, based on our simulations, the dipolar term of the hyperfine interaction should be close to zero as far as the local symmetry is preserved, but the accuracy of our calculations does not allow us to provide detailed data to be compared with experiments.

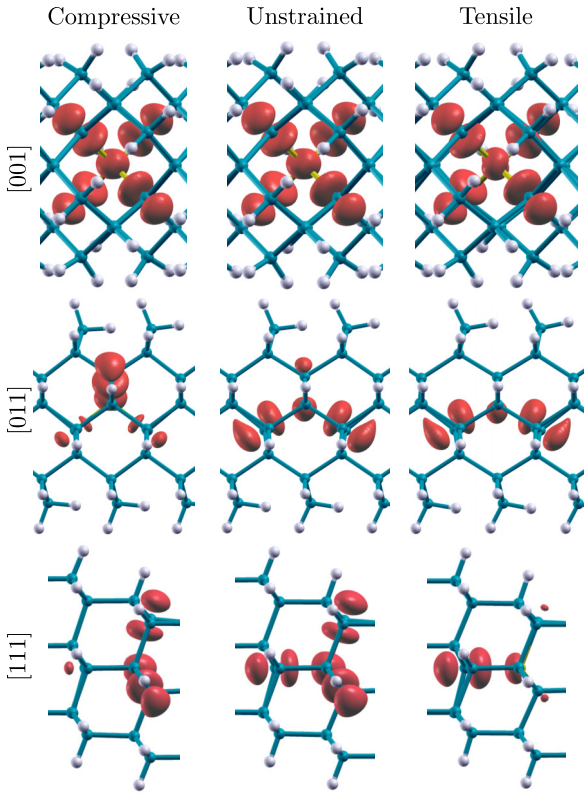

FIG. 4. (Color online) Side view of the spin densities isosurfaces $n_s(\mathbf{r})$ in the smallest Se doped SiNWs considered, for [001] (top), [011] (middle), and [111] (bottom) orientations. The nanowires are under a compressive strain in the left columns (namely -2% for [001] and [111], and -4% for [011]), in the unstrained configuration in the middle and under a $+2\%$ tensile strain on the right. The spin density isosurface correspond to an isovalue of 0.014 $e/$Å

We will now examine in detail the effect of uniaxial strain on the spin density $n_s(\mathbf{r})$ and, consequently, on the hyperfine parameters. To this aim, the calculated $n_s(\mathbf{r})$ for the compressed, unstrained, and tensed nanowires are shown in Fig. 4. The isosurfaces are shown at intermediate values of the strain to highlight the effects in a region that should be more easily achieved experimentally and to show how effective a small strain could be in changing the shape of the spin density. Note that $n_s(\mathbf{r})$ is always almost equivalent to the defect level wave function.

For [001] oriented nanowires, applying a strain slightly breaks the local tetrahedral symmetry of the defect, by changing the relative angles but keeping the bonds between the impurity and its nearest neighbors of the same length. As a consequence, the main change of the spin density is the orientation of the lobes with respect to the axis of the nanowire, while its amount in the neighborhood of the nuclei remains almost constant. This can be seen quantitatively in Fig. 3, where a and the SHFI of the nearest neighbor a_{shf} show only very small variations and just when a large strain is applied a sizable change can be observed, although still quite small compared to the other orientations. Here the b term depends on the tilting of the spin density distribution with respect to the

nanowire axis and changes linearly in the range considered. Here, as for the following cases, the decrease of b for an increasing tensile strain is mainly driven by the deformation of the spin density close to the defect: elongated along the axis, when the nanowires are compressed, and flattened in the xy plane, when the nanowires are tensed [45].

The situation is different for the other two orientations, since the strain acts nonuniformly on the four defect bonds and strongly breaks the local symmetry. Both for [011] and [111] nanowires the overall effect is given by the action of the strain on the bonds that are approximately oriented along the axis. When the nanowire is compressed and these bonds are reduced, the spin density is progressively repelled from their neighborhood and localizes on the bonds perpendicular to the nanowire axis. On the contrary, when a tensile strain is applied, the bonds parallel to the axis are elongated and the spin density is localized there, emptying the region close to the other bonds. This is immediately evident from the spin densities shown Fig. 4.

From a quantitative point of view, this can be verified studying the a_{shf} terms in Fig. 3. Their values for the atoms displaced along the axis of the nanowire ($\mathrm{Si}_{\parallel z}$) have an opposite trend compared to those for the atoms that have a Se-Si bond in a plane perpendicular to the axis ($\mathrm{Si}_{\perp z}$). Under tensile strain a_{shf} tends to zero for $\mathrm{Si}_{\perp z}$ and for $\mathrm{Si}_{\parallel z}$ can be as large as 207 MHz, while the situation is reversed for compressive strain. Notably, at the crossing point, a_{shf} has a value of approximately 54 MHz for both [011] and [111] nanowires, matching with high accuracy those found for the [001] nanowire in the whole range of strain considered. This point corresponds to the most symmetric configuration of the spin density, and, as a consequence, matches the strain at which the defect hyperfine contact term a is at its maximum. The superhyperfine dipolar terms b_{shf} follow quite uniformly the trends of the respective a_{shf}, further confirming the picture outlined above.

It is important to note that in this configuration even the value of a is approximately the same for all the three orientations (around 2030 MHz). This shows once again that the hyperfine parameters in nanowires of the same diameters are orientation dependent only as long as the different orientations lead to different local symmetry breakings. All the deviations from a common trend in Fig. 2 should thus be mainly ascribed to a lowering of the local symmetries in the relaxed geometry.

In the case of the [011] nanowire the maximum symmetry is achieved for a compressive strain of -3%. This is a consequence of the strain induced by the passivating H atoms for the nanowire considered and such a high value should not be expected for all the other [011] configurations. Nonetheless, [011] orientation favors a delocalization of the donor wave function and the maximum values should be reached under compression.

When departing from the symmetric configuration, the shift of the spin density can lead to a fast decrease of the a value that can reach a linear regime as a function of the applied strain. This strong variations under applied strain, together with fast large changes in the delocalization of the donor wave function, confirms the doped [011] nanowires as good candidates for strain controlled spin qubits [31].

This behavior can also suggest that an applied external strain can also contribute to reverting the symmetry breakings in S doped nanowires discussed in Sec. III.

As an additional point, we highlight that, close to the unstrained system, even for [011] and [111] oriented nanowires the anisotropic term b has a linear dependence on the applied strain, but with a larger slope compared to [001] nanowires. It approaches zero at the point of maximum symmetry, but can be sizable when a large strain is applied, due to the quite relevant deformation of the spin density, as shown in Fig. 3.

Lastly, it is interesting to point out that no saturation of the contact term a is observed in the explored strain range, while a sign of convergence can be observed for some of the other parameters in [011] and [111] nanowires. In the case of a_{shf} this is a consequence of the spin density being more delocalized and the increase of hyperfine terms for further Si atoms.

V. CONCLUSIONS

In this work we have considered Se and S doped SiNWs and GeNWs and analyzed the dependence of hyperfine parameters on nanowires diameter and orientation. We have shown that only a small dependence on the orientation and a linear dependence on the diameter is present in the hyperfine contact term a for Se doped nanowires. At variance, the S defect tends to distort the local symmetry more easily, making the results more dependent on the specific nanowire configuration. In addition, we have studied the effect of compressive and tensile uniaxial strain in the representative case of Se doped SiNWs with different orientations. This contributed to assessing the reliability of our calculations and allowed us to observe the possibility of tuning a for different orientations. Based on these results, we confirm the [011] oriented nanowires as promising candidates for spin qubits applications, in particular if strain manipulation is considered.

ACKNOWLEDGMENTS

The research activity presented here is performed in the framework of the ELIOS research project, which is supported by Fondazione Cariplo. We acknowledge CASPUR consortium providing computational resources for the project "Chalcogen Impurities in Si-NAnowires (CISNA)" and CINECA computational resources under the project "Chalcogen Impurities in Si and Ge Nanowires (CISIGEN)." Computational resources have also been provided by the supercomputing facilities of the Université catholique de Louvain (CISM/UCL) and the Consortium des Équipements de Calcul Intensif en Fédération Wallonie Bruxelles (CÉCI) funded by the Fond de la Recherche Scientifique de Belgique (FRS-FNRS).

[1] M. S. Gudiksen, L. J. Lauhon, J. Wang, D. C. Smith, and C. M. Lieber, Nature (London) **415**, 617 (2002).

[2] Y. Cui, Z. Zhong, D. Wang, W. U. Wang, and C. M. Lieber, Nano Lett. **3**, 149 (2003).

[3] C. M. Cui and Y. Lieber, Science **291**, 851 (2001).
[4] X. Duan, Y. Huang, Y. Cui, J. Wang, and C. M. Lieber, Nature (London) **409**, 66 (2001).
[5] X. Duan, Y. Huang, R. Agarwal, and C. M. Lieber, Nature (London) **421**, 241 (2003).
[6] B. Tian, X. Zheng, T. J. Kempa, Y. Fang, N. Yu, G. Yu, J. Huang, and C. M. Lieber, Nature (London) **449**, 885 (2007).
[7] T. J. Kempa, B. Tian, D. R. Kim, J. Hu, X. Zheng, and C. M. Lieber, Nano Lett. **8**, 3456 (2008).
[8] M. Fanciulli, A. Vellei, C. Canevali, S. Baldovino, G. Pennelli, and M. Longo, Nanosci. Nanotechnol. Lett. **3**, 568 (2011).
[9] M. Fanciulli, A. Molle, S. Baldovino, and A. Vellei, Microelectron. Eng. **88**, 1482 (2011).
[10] R. Rurali, Rev. Mod. Phys. **82**, 427 (2010).
[11] A. N. Kholod, V. L. Shaposhnikov, N. Sobolev, V. E. Borisenko, F. A. D'Avitaya, and S. Ossicini, Phys. Rev. B **70**, 035317 (2004).
[12] A. J. Lee, T.-L. Chan, and J. R. Chelikowsky, Phys. Rev. B **89**, 075419 (2014).
[13] M. Amato, M. Palummo, R. Rurali, and S. Ossicini, Chem. Rev. **114**, 1371 (2014).
[14] M. Amato, S. Ossicini, and R. Rurali, Nano Lett. **11**, 594 (2011).
[15] B. E. Kane, Nature (London) **393**, 133 (1998).
[16] B. E. Kane, N. S. McAlpine, A. S. Dzurak, R. G. Clark, G. J. Milburn, H. B. Sun, and H. Wiseman, Phys. Rev. B **61**, 2961 (2000).
[17] B. Yan, R. Rurali, and A. Gali, Nano Lett. **12**, 3460 (2012).
[18] D. V. Melnikov and J. R. Chelikowsky, Phys. Rev. Lett. **92**, 046802 (2004).
[19] A. Debernardi and M. Fanciulli, Solid State Sci. **11**, 961 (2009).
[20] A. Debernardi and M. Fanciulli, Phys. Rev. B **81**, 195302 (2010).
[21] M. Fujii, A. Mimura, S. Hayashi, Y. Yamamoto, and K. Murakami, Phys. Rev. Lett. **89**, 206805 (2002).
[22] R. Rurali, B. Aradi, T. Frauenheim, and A. Gali, Phys. Rev. B **79**, 115303 (2009).
[23] G. Petretto, A. Debernardi, and M. Fanciulli, Nano Lett. **11**, 4509 (2011).
[24] G. P. Berman, G. D. Doolen, P. C. Hammel, and V. I. Tsifrinovich, Phys. Rev. Lett. **86**, 2894 (2001).
[25] P. Giannozzi, S. Baroni, N. Bonini, M. Calandra, R. Car, C. Cavazzoni, D. Ceresoli, G. L. Chiarotti, M. Cococcioni, I. Dabo *et al.*, J. Phys.: Condens. Matter **21**, 395502 (2009).
[26] J. P. Perdew, K. Burke, and M. Ernzerhof, Phys. Rev. Lett. **77**, 3865 (1996).
[27] J. P. Perdew and A. Zunger, Phys. Rev. B **23**, 5048 (1981).
[28] M. S. Hybertsen and S. G. Louie, Phys. Rev. B **30**, 5777 (1984).
[29] I. N. Remediakis and E. Kaxiras, Phys. Rev. B **59**, 5536 (1999).
[30] Y. M. Niquet, L. Genovese, C. Delerue, and T. Deutsch, Phys. Rev. B **81**, 161301 (2010).
[31] G. Petretto, A. Debernardi, and M. Fanciulli, Nano Lett. **13**, 4963 (2013).
[32] N. Troullier and J. L. Martins, Phys. Rev. B **43**, 1993 (1991).
[33] C. G. Van de Walle and P. E. Blöchl, Phys. Rev. B **47**, 4244 (1993).
[34] C. J. Pickard and F. Mauri, Phys. Rev. Lett. **88**, 086403 (2002).
[35] H. J. Monkhorst and J. D. Pack, Phys. Rev. B **13**, 5188 (1976).
[36] T. Vo, A. J. Williamson, and G. Galli, Phys. Rev. B **74**, 045116 (2006).
[37] T.-L. Chan, C. V. Ciobanu, F.-C. Chuang, N. Lu, C.-Z. Wang, and K.-M. Ho, Nano Lett. **6**, 277 (2006).
[38] E. Koren, J. K. Hyun, U. Givan, E. R. Hemesath, L. J. Lauhon, and Y. Rosenwaks, Nano Lett. **11**, 183 (2011).
[39] S. Gruelich-Weber, J. R. Niklas, and J. M. Spaeth, J. Phys. C: Solid State Phys. **17**, L911 (1984).
[40] G. W. Ludwig, Phys. Rev. **137**, A1520 (1965).
[41] L. Dreher, T. A. Hilker, A. Brandlmaier, S. T. B. Goennenwein, H. Huebl, M. Stutzmann, and M. S. Brandt, Phys. Rev. Lett. **106**, 037601 (2011).
[42] G. Pfanner, C. Freysoldt, and J. Neugebauer, Phys. Rev. B **83**, 144110 (2011).
[43] G. Pfanner, C. Freysoldt, J. Neugebauer, and U. Gerstmann, Phys. Rev. B **85**, 195202 (2012).
[44] R. Minamisawa, M. Süess, R. Spolenak, J. Faist, C. David, J. Gobrecht, K. Bourdelle, and H. Sigg, Nature Commun. **3**, 1096 (2012).
[45] G. Petretto, Ph.D. thesis, Università degli Studi di Milano-Bicocca, 2012.